J Pharmacol Sci **104**, 341 – 348 (2007)

Journal of Pharmacological Sciences

Full Paper

Edaravone Preserves Coronary Microvascular Endothelial Function After Ischemia/Reperfusion on the Beating Canine Heart In Vivo

Renan Sukmawan[1,*], Toyotaka Yada[2], Eiji Toyota[1], Yoji Neishi[1], Teruyoshi Kume[1], Yoshiro Shinozaki[3], Hidezo Mori[4], Yasuo Ogasawara[2], Fumihiko Kajiya[2], and Kiyoshi Yoshida[1]

Departments of [1]Cardiology and [2]Medical Engineering and Systems Cardiology, Kawasaki Medical School, Kurashiki 701-0192, Japan
[3]Department of Physiology, Tokai University School of Medicine, Isehara 259-1193, Japan
[4]Department of Cardiac Physiology, National Cardiovascular Center Research Institute, Suita 565-8565, Japan

Received January 22, 2007; Accepted June 13, 2007

Abstract. We examined whether edaravone (3-methyl-1-phenyl-2-pyrazolin-5-one), a free radical scavenger, exerts its protective effect on coronary microvessels after ischemia/reperfusion (I/R) in vivo. Ninety-minute coronary occlusion followed by reperfusion was performed in 16 open-chest dogs with and without edaravone administration. Coronary small artery (≥100 μm in size) and arteriolar (<100 μm) vasodilation, in the presence of endothelium-dependent (acetylcholine) or -independent (papaverine) vasodilators, was directly observed using intravital microscopy before and after I/R. I/R impaired microvascular vasodilation in response to acetylcholine, whereas administration of edaravone preserved the response in microvessels of both sizes, but to a greater extent in the coronary small arteries. No significant changes were noted with papaverine administration. In the edaravone group, the fluorescent intensity from reactive oxygen species (ROS) was lower, whereas nitric oxide (NO) intensity was higher relative to controls in the microvessels of the ischemic area. In conclusion, edaravone preserves coronary microvascular endothelial function after I/R in vivo. These effects, which were NO-mediated, were attributed to the ROS scavenging properties of edaravone.

Keywords: coronary microvessel, edaravone, ischemia/reperfusion, reactive oxygen species, nitric oxide (NO)

Introduction

Coronary microvessels play a pivotal role in the regulation of coronary blood flow (1, 2). Dysfunction of coronary microvessels, especially the resistance vessels, has been associated with an increase in future cardiovascular events in patients with coronary diseases (3, 4). Even in normal subjects, coronary microvascular dysfunction has been shown to increase the risk for a cerebrovascular event (5).

Ischemia/reperfusion (I/R) may result in microvascular dysfunction that further attenuates cardiac functional recovery (6 – 8). One of the central mechanisms responsible for the adverse effect of I/R is free radical production, which includes reactive oxygen species (ROS) (9, 10). A burst of ROS is generated during ischemia and in early reperfusion. This burst overwhelms the antioxidant defense band and causes disturbance in the cardiovascular system (11, 12).

Edaravone (3-methyl-1-phenyl-2-pyrazolin-5-one), a potent free radical scavenger, has been shown to protect cardiomyocytes and brain against I/R injury (13, 14). However, the beneficial effects on coronary microcirculation after I/R remains unknown. We sought to define the effects of edaravone on coronary microvessels after I/R in vivo by 1) direct observation of endothelium-dependent and -independent vasodilation of subepicardial coronary microvessels on the beating canine heart using a charged couple device (CCD) intravital microscope and 2) In-situ detection of ROS and

*Corresponding author. Present address: Department of Cardiology and Vascular Medicine, University of Indonesia / National Cardiovascular Center, Jalan Letjen S Parman Kav 87, Jakarta 11420, Indonesia rey1708@yahoo.com
Publihshed online in J-STAGE
doi: 10.1254/jphs.FP0070186

nitric oxide (NO) in coronary microvessels.

Material and Methods

Animal preparation

We conformed to the Guideline on Animal Experiments and the Guide for the Care and Use of Laboratory Animals published by the National Institutes of Health (NIH) of the United States and the Guiding Principles for the Care and Use of Laboratory Animals approved by the Japanese Pharmacological Society. Sixteen adult mongrel dogs of either sex (15 – 24 kg; purchased from Nagoyalab Service, Mizunami) were premedicated with ketamine (10 mg/kg, i.m.) and anesthetized with sodium pentobarbital (25 mg/kg, i.v.). Each animal was intubated and mechanically ventilated (model VS-600; Instrumental Development, Pittsburgh, PA, USA) with 2% – 3% fluorethane. Blood gas and oxygen saturation were controlled within physiologic ranges throughout the experiment. Open-chest surgery was performed by medial sternotomy and the left anterior descending artery (LAD) was isolated free from surrounding tissue at proximal and medial portions. A transonic flow probe (T206; Transonic Systems, Ithaca, NY, USA) was placed at the medial portion of the LAD to measure the coronary flow rate. A clamp was placed at the proximal LAD to produce coronary occlusion and reperfusion. Visible native collateral vessels were ligated to limit collateral flow into the ischemic area during LAD occlusion. A 6F-catheter was inserted into the right carotid artery through the left coronary artery to administer the vasodilator.

Experimental protocols

After instrumentation, a minimum of 30 min were allowed for stabilization while monitoring hemodynamic variables. The study protocol was as follows: i) The arteriolar vasodilatory response to endothelium-dependent (acetylcholine, 1 μg/kg, i.c.; Daiichi Pharmaceutical Co., Ltd., Tokyo) and -independent (papaverine, 1 mg, i.c.; Dainippon Sumitomo Pharma Co., Ltd., Osaka) vasodilators were examined before and after coronary I (90 min) /R (60 min) under the following conditions: a) control condition, and b) edaravone administration (3 mg/kg, i.v.; supplied by Mitsubishi Pharma Co., Ltd., Osaka) before coronary occlusion. Microspheres were administered at 85 min of coronary occlusion to measure regional myocardial blood flow (MBF). ii) Fluorescent treatment to assess microvascular ROS and NO were performed in 6 dogs (n = 3, each group) after a 60-min reperfusion period. iii) In another 10 dogs (n = 5, each), reperfusion was continued for 5 h and the infarct size and regional MBF were measured.

Intravital CCD microscopy

Direct observation of coronary microvascular vasodilation on the beating heart was performed by using a needle-probe intravital CCD microscope (VMS 1210; Nihon Kohden, Tokyo). It contains a gradient index lens (with a magnification of 200) surrounded by light guide fibers and a double lumen sheath. To avoid direct compression of the vessels by the needle-tip, a doughnut-shaped balloon had been installed (15). Vascular images were acquired by gently placing the needle-probe on subepicardial microvessels and were recorded at 30 frames/s. Off-line quantitative analysis was performed using an NIH image analysis software by measuring maximum diameter changes during acetylcholine or papaverine administration.

In situ detection of ROS and NO in coronary microvessels

After reperfusion, the heart was immediately removed. The LAD orifice and left circumflex (LCX) artery were cannulated for a continuous phosphate-buffered saline (PBS) infusion. Small tissue blocks were taken from both ischemic (LAD area) and non-ischemic regions (LCX area), and they were frozen in optimal cutting temperature compound (Tissue-Tek; Sakura Fine Chemical, Tokyo) within a few hours. Fluorescent images of the microvessels were obtained using a fluorescent microscope (Olympus BX 51; Olympus, Tokyo). Dihydroethidium (DHE; Molecular Probes, Eugene, OR, USA) and 4,5-diaminofluorescein diacetate (DAF-2DA; Daiichi Pure Chemicals, Tokyo) were used to detect ROS and NO production, respectively (16). Five regions of interest (ROI) were selected within the intimal layer of each microvessel. Fluorescent intensities of ROS and NO in the microvessels were measured by NIH software. The average value of the peak fluorescent intensity from each ROI was divided by background intensity (relative intensity) and noted as the microvascular ROS or NO intensities.

Western blotting

Myocardial tissue samples from the LAD and LCX area in each group were isolated for western blotting to assess endogenous NO synthase (eNOS) protein expression after I/R, as previously described (8, 16). Briefly, myocardial tissues were homogenized in the lysis buffer. After centrifugation, the supernatant was collected for immunoblotting. The proteins were transferred by semi-dry electroblotting to polyvinylidene difluoride membranes. The blots were then blocked and incubated with rabbit anti-eNOS polyclonal antibody (0.1 μg/ml; Santa Cruz Biotechnology, Santa Cruz, CA, USA) or anti-actin antibody (Santa Cruz Biotechnology) for 120 min

at room temperature. The blots were then incubated with horseradish peroxidase-conjugated goat anti-rabbit IgG (0.08 μg/ml, Santa Cruz Biotechnology). The antibody was visualized using an enhanced chemiluminescence method (ECL; Amersham Biosciences, Piscataway, NJ, USA). The integrated density of the eNOS bands was normalized by actin band density (relative density) (NIH Image).

Regional blood flow and infarct size

To confirm infarct size reduction by edaravone in relation to the effect of collateral flow, regional MBF was assessed by non-radioactive microspheres (Sekisui Plastic Co., Ltd., Tokyo), as previously described (17). Briefly, 1 ml of the microsphere suspension (2 to 4 × 10^6 spheres) was injected into the left atrium 85 min after the onset of coronary occlusion. MBF was measured by assessing X-ray spectra of the fluorescent stable heavy elements using a wavelength-dispersive spectrometer (model PW 1480; Philips Co., Ltd., Eindhoven, the Netherlands). Myocardial collateral flow (ml/min per gram) was calculated using the following formula: tissue flow-rate = tissue counts × (reference flow / reference counts).

Myocardial short-axis slices (5-mm-thickness) of the left ventricle were made and incubated in 1% 2,3,5-triphenyltetrazoliumchloride solution (Sigma, Tokyo) for 10 min to identify the infarct area. Infarct size was expressed as a percentage of the infarct area relative to the area of risk (18).

Statistical analysis

Data are expressed as the mean ± S.E.M. The vascular response was analyzed by one-way analysis of variance followed by a Scheffe's post-hoc test for multiple comparisons (Figs. 1C, 2, 3, and 4). Regression analysis was applied in Fig. 5. Statistical significance was defined as $P<0.05$.

Results

Hemodynamics

Hemodynamic data are shown in Table 1. Mean arterial pressure and heart rate during administration of acetylcholine and papaverine were not statistically different as compared to their respective baseline. Hemodynamic variables at baseline did not significantly change before and after I/R nor after edaravone administration.

Endothelium-dependent vasodilation

We assessed the diameter changes of 22 coronary microvessels under acetylcholine (1 μg/kg, i.c.) in each group. The diameter changes of small artery and arteriole in each group are depicted in Fig. 1, A and B. Under control conditions (without edaravone), I/R strikingly impaired endothelium-dependent vasodilation at 60 min after I/R. Meanwhile, edaravone administration augmented the response in coronary microvessels of both sizes. Preservation of vasodilation under acetylcholine was more prominent in the small artery than the arteriole. Coronary flow in the presence of acetylcholine was improved after I/R in the edaravone-adminstered group compared with that in the controls (without edaravone) (Fig. 1C).

ROS intensity in coronary microvessels

Fifteen coronary microvessels (<300 μm) were assessed from both the LAD and LCX areas in both groups (Fig. 2). ROS fluorescent intensity at 60 min after I/R in the microvessels from the LAD area in the control group was higher than in the LCX area ($P<0.01$). Meanwhile, ROS intensity in the microvessels from the LAD area of the edaravone group was significantly lower than that in the control group ($P<0.01$).

Intensity of NO in coronary microvessels

Fluorescent intensity of NO in the endothelial layer was assessed semi-quantitatively in 15 microvessels from the LAD or LCX areas in both groups 60 min after

Table 1. Hemodynamics data before and after ischemia/reperfusion

	Before I/R			After I/R		
	Baseline	Acetylcholine	Papaverine	Baseline	Acetylcholine	Papaverine
Mean blood pressure (mmHg)						
Control	91 ± 4	90 ± 6	91 ± 4	89 ± 4	89 ± 5	87 ± 5
Edaravone	92 ± 2	91 ± 4	90 ± 3	93 ± 3	91 ± 5	90 ± 4
Heart rate (beats/min)						
Control	123 ± 5	125 ± 3	126 ± 4	120 ± 4	122 ± 5	120 ± 5
Edaravone	124 ± 4	126 ± 6	123 ± 5	123 ± 4	121 ± 5	120 ± 4

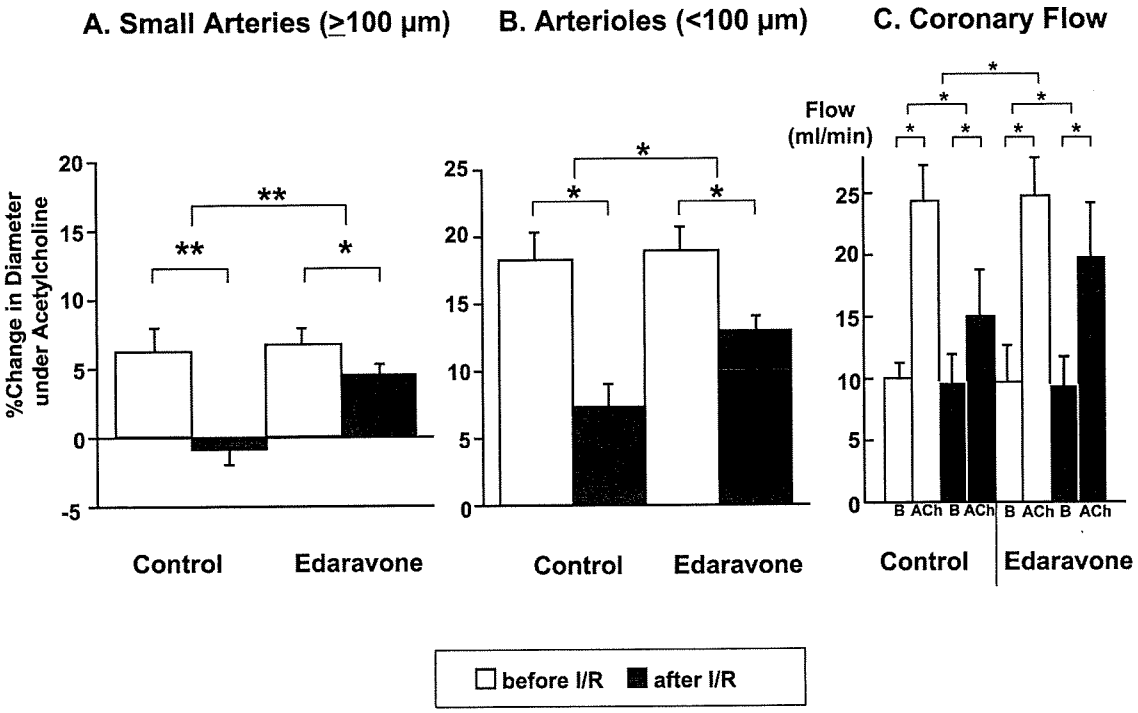

Fig. 1. Endothelium-dependent vasodilation in coronary microvessels in vivo. Edaravone administration augmented the vasodilation of small arteries (A) and arterioles (B) and improved coronary flow (C) under acetylcholine after I/R. Number of small arteries and arterioles assessed were 10 and 12, respectively. *P<0.05, **P<0.01. B = baseline, ACh = acetylcholine.

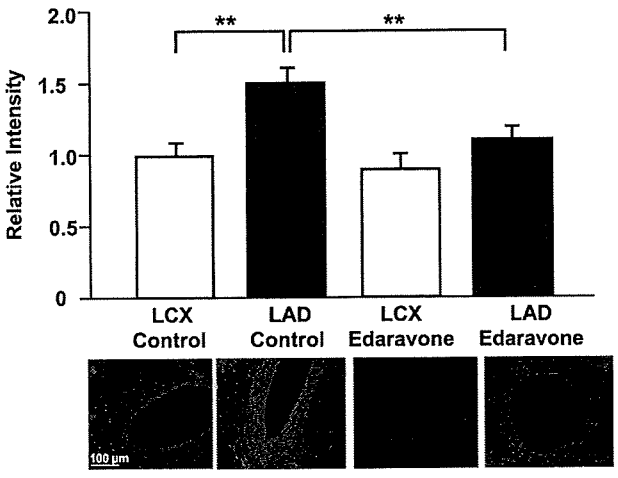

Fig. 2. In situ detection of ROS in coronary microvessels after I/R. The fluorescent intensity of ROS in microvessels from each area is shown (n = 15, in each area) with their representative DHE-fluorescence image of ROS in the vessels. **P<0.01.

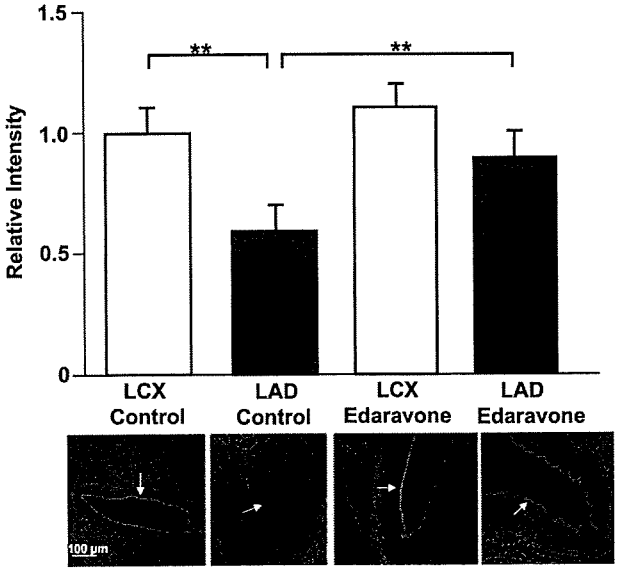

Fig. 3. In situ detection of NO in coronary microvessels after I/R. Fluorescent intensity of NO in microvessels from each area is shown (n = 15, in each area) with their representative DAF2-DA fluorescence image of NO in the endothelial layer (white arrow). **P<0.01.

I/R (Fig. 3). In the LAD area of the control group (without edaravone), I/R reduced the microvascular NO intensity level as compared to the LCX area (P<0.01). Administration of edaravone significantly preserved NO

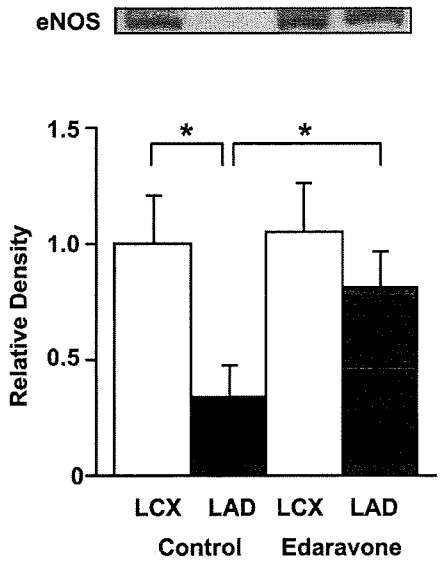

Fig. 4. eNOS protein immunoblotting after I/R. Edaravone administration augmented myocardial eNOS expression after I/R in the ischemic area. *P<0.05.

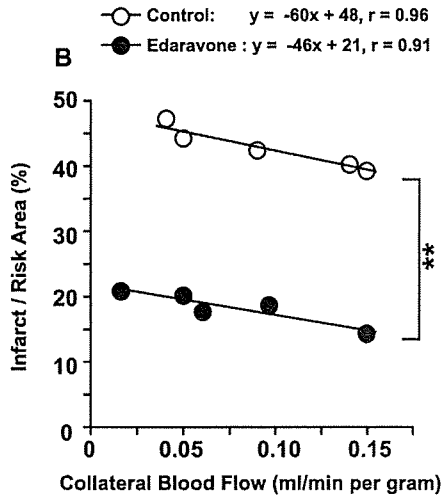

Fig. 5. Correlation of regional collateral flow and infarct size in the control and edaravone groups. **P<0.01.

fluorescent intensity in microvessels of LAD relative to the control group (P<0.01).

Myocardial eNOS expression

Myocardial eNOS protein expression in the LAD distribution after I/R was significantly decreased relative to the LCX area in the control group (without edaravone, P<0.05, Fig. 4). Edaravone augmented eNOS protein expression in the LAD area (P<0.05 *vs* controls).

Collateral flow and infarct size

There were linear negative correlations between regional collateral MBF and infarct size in the control ($y = -60X + 48$, $r = 0.96$, P<0.001) and edaravone ($y = -46X + 21$, $r = 0.91$, P<0.001) groups, which were significantly different between the 2 groups (P<0.01, Fig. 5). This finding indicated that the protective effect of edaravone was independent of collateral flow.

Endothelium-independent vasodilation

Endothelium-independent vasodilation with papaverine (1 mg, i.c.) was comparable under all conditions (Fig. 6). Administration of edaravone did not result in any significant diameter changes in small arteries and arterioles under papaverine after I/R.

Discussion

The present study revealed that edaravone preserves endothelium-dependent vasodilation in coronary small arteries and arterioles after I/R injury on the beating canine heart in vivo by reducing ROS and thereby augmenting NO availability in the microvessels. To our knowledge, the present study is the first to report that edaravone exerts protective effects on the coronary microvascular endothelial function after I/R on the beating heart in vivo.

Scavenging ROS by edaravone during ischemia/reperfusion

Generation of ROS during I/R has been shown through several mechanisms such as the xanthine oxidase, mitochondrial electron transport chain, and NADPH oxidase pathways (10). In the present study, we revealed that edaravone scavenged ROS generated in coronary microvessels during I/R (Fig. 2). Previous studies have shown other beneficial effects of edaravone such as inhibition of the production of superoxide anion on the infarct rim (14), suppression of lipid peroxidation products (19), and reduction in inflammatory changes (20).

The burst of vascular ROS production following I/R led to endothelial dysfunction, which may have occurred as a result of hypoxic injury, manifested by endothelial cell swelling that results in the no reflow phenomenon within the first minutes of reperfusion (21). The ROS may also rapidly react with NO to form a toxic peroxynitric radical (i.e., $ONOO^-$) that further increases free radical accumulation resulting in endothelial injury (9). If the ischemia lasts for hours, structural changes such as edematous mitochondria in endothelial and smooth muscle cells, microvili formation on the surface of endothelial cells, and increased pinocytic activity and

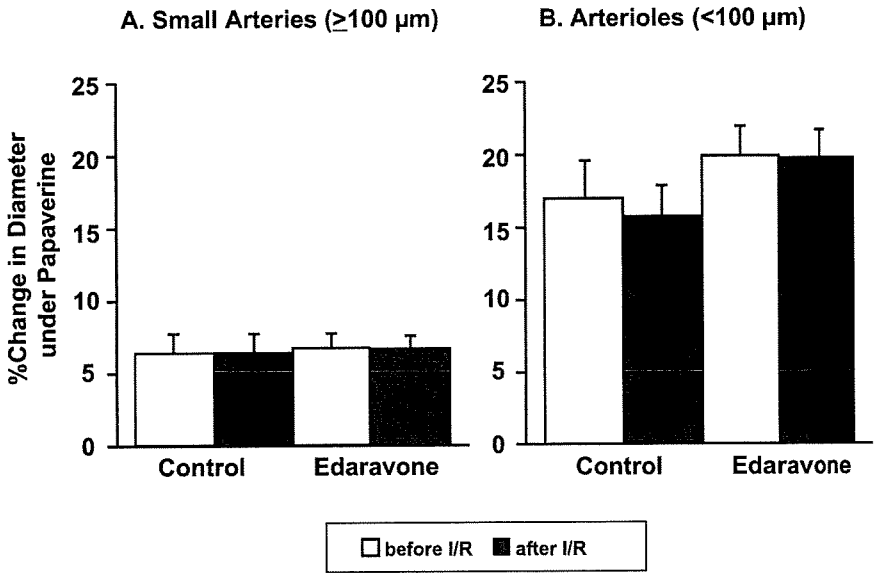

Fig. 6. Endothelium-independent vasodilation in coronary microvessels before and after I/R. The vasodilation is comparable under all conditions.

disturbed tight junctions between endothelial cells may be found by electronmicroscopical examination (21). With edaravone administration, NO bioavailability in the ischemic area endothelial layer of microvessels was significantly augmented (Fig. 3). In other settings, edaravone has also been shown to improve peripheral flow-mediated dilatation in smokers (22). Taken together, free radical scavenging by edaravone in the vessels results in preservation of NO availability and thereby maintains endothelial function, which is crucial for the cardiovascular system in both the short-term and long-term.

Edaravone preserves nitric oxide and eNOS

We have previously shown that endothelium-dependent vasodilation by acetylcholine would increase NO release in coronary circulation, indicating the central role of NO (23). However, the regulation of coronary vascular tone may be mediated, not only by NO, but also by the endothelium derived hyperpolarizing factor (EDHF) and adenosine (24). Yada et al. have demonstrated that endogeneous H_2O_2, an EDHF, and rho-kinase inhibition mediated coronary vasodilation to a greater extent in arterioles than in small arteries (7, 8, 24). In the present study, preservation of endothelium-dependent vasodilation by edaravone was noted to a greater extent in the small arteries (Fig. 1). These facts revealed various mechanisms and 'site-specific' action of different drugs or agents in the coronary circulation. These also indicated a predominant role of NO in small arteries, as opposed to arterioles. Taken together, the protective effects of NO and EDHF in coronary microvessels during I/R may occur in a compensatory manner.

Most of the NO production in the normal heart is accounted for by the presence of nitric-oxide synthase (eNOS) in the coronary endothelium and myocardium. Impaired NO synthesis from eNOS is a mechanism of endothelial dysfunction in the post-ischemic heart. The present study demonstrated reduced eNOS protein expression in the ischemic myocardium after I/R, whereas edaravone administration preserved the expression (Fig. 4). Previous studies from our institution have also demonstrated a decrease in eNOS protein expression in ischemic myocardium following I/R (7, 8). An in vitro study in HUVEC has shown that edaravone may increase eNOS expression via the inhibition of LDL oxidation (25). Thus, the burst of ROS generation during I/R may cause cell injury that results in reduced eNOS production, and edaravone administration preserves the eNOS expression.

Myocardial protection by edaravone

The present study confirmed the protective effect of edaravone on the myocardial cell (13) and revealed that the cardioprotective role of edaravone during I/R was irrespective of transmural collateral flow to the ischemic area (Fig. 5). It has been hypothesized that maintenance of endothelium-dependent dilation of coronary microvessels could enhance reperfusion damage and reduces the amount of tissue necrosis (26). Thus, preservation of microvascular endothelial function

by edaravone probably contributed to the improvement in myocardial perfusion, thereby facilitating myocardial tissue preservation after I/R.

In the present study, we administered edaravone prior to coronary occlusion because ROS generation may occur during occlusion and after reperfusion. Wu et al. have shown a protective effect of edaravone on the myocardium when it was administered during coronary occlusion or after reperfusion (27). Thus, we presumed that preservation of endothelial function by edaravone may also be observed if it is administered during occlusion or after reperfusion. Nevertheless, further study is needed to confirm these issues.

Conclusions

In conclusion, edaravone exerts beneficial protective effects on coronary microvessels by preserving endothelial function after I/R in vivo. These effects are attributed to the ROS scavenging properties of edaravone and involves an NO-mediated mechanism.

Acknowledgments

This work was supported in part by a grant (No 16300164) from the Japanese Ministry of Education, Science, Sports, Culture, and Technology and a grant from the program for promotion of fundamental studies in health sciences of the Organization for Pharmaceutical Safety and Research in Japan.

References

1 Chilian WM, Kuo L, DeFily DV, Jones CJ, Davis MJ. Endothelial regulation of coronary microvascular tone under physiological and pathophysiological conditions. Eur Heart J. 1993;1 Suppl I:55–59.

2 Kuo L, Davis MJ, Chilian WM. Endothelium-dependent, flow-induced dilation of isolated coronary arterioles. Am J Physiol. 1990;259:1063–1170.

3 Suwaidi JA, Hamasaki S, Higano ST, Nishimura RA, Holmes DR, Lerman A. Long-term follow-up of patients with mild coronary artery disease and endothelial dysfunction. Circulation. 2000;101:948–954.

4 Schächinger V, Britten B, Zeiher AM. Prognostic impact of coronary vasodilator dysfunction on adverse long-term outcome of coronary heart disease. Circulation. 2000;101:1899–1906.

5 Targonski PV, Bonetti PO, Pumper GM, Higano ST, Holmes DR, Lerman A. Coronary endothelial dysfunction is associated with an increased risk of cerebrovascular events. Circulation. 2003;107:2805–2809.

6 Matsumura K, Jeremy RW, Schaper J. Progression of myocardial necrosis during reperfusion of ischemic myocardium. Circulation. 1998;97:795–804.

7 Yada T, Shimokawa H, Hiramatsu O, Kajita T, Shigeto F, Tanaka E, et al. Beneficial effect of hydroxyfasudil, a specific Rho-kinase inhibitor, on ischemia/reperfusion injury in canine coronary microcirculation in vivo. J Am Coll Cardiol. 2005;45:599–607.

8 Yada T, Shimokawa H, Hiramatsu O, Haruna Y, Morita Y, Kashihara N, et al. Cardioprotective role of endogenous hydrogen peroxide during ischemia-reperfusion injury in canine coronary microcirculation in vivo. Am J Physiol Heart Circ Physiol. 2006;291:H1138–1146.

9 Bolli R, Jeroudi MO, Patel BS, DuBose CM, Lai EK, Roberts R, et al. Direct evidence that oxygen-derived free radicals contribute to postischemic myocardial dysfunction in the intact dog. Proc Natl Acad Sci U S A. 1989;86:4695–4699.

10 Zweier JL, Talukder MA. The role of oxidants and free radicals in reperfusion injury. Cardiovasc Res. 2006;70:181–190.

11 Becker LB, vanden Hoek TL, Shao ZH, Li CQ, Schumacker PT. Generation of superoxide in cardiomyocytes during ischemia before reperfusion. Am J Physiol. 1999;277:H2240–H2246.

12 Kevin LG, Camara AK, Riess ML, Novalija E, Stowe DF. Ischemic preconditioning alters real-time measure of O_2 radicals in intact hearts with ischemia and reperfusion. Am J Physiol Heart Circ Physiol. 2003;284:H566–H574.

13 Yamawaki M, Sasaki N, Shimoyama M, Miake J, Ogino K, Igawa O, et al. Protective effect of edaravone against hypoxia-reoxygenation injury in rabbit cardiomyocytes. Br J Pharmacol. 2004;142:618–626.

14 Shichinohe H, Kuroda S, Yasuda H, Ishikawa T, Iwai M, Horiuchi M. Neuroprotective effects of the free radical scavenger edaravone (MCI-186) in mice permanent focal brain ischemia. Brain Res. 2004;1029:200–206.

15 Yada T, Hiramatsu O, Kimura A, Goto M, Ogasawara Y, Tsujioka K. In vivo observation of subendocardial microvessels of the beating porcine heart using a needle-probe video-microscope with a CCD camera. Circ Res. 1993;72:939–946.

16 Satoh M, Fujimoto S, Haruna Y, Arakawa S, Horike H, Komai N, et al. NAD(P)H oxidase and uncoupled nitric oxide synthase are major sources of glomerular superoxide in rats with experimental diabetic nephropathy. Am J Physiol Renal Physiol. 2005;288:F1144–F1152.

17 Mori H, Haruyama S, Shinozaki Y, Okino H, Iida A, Takanashi R, et al. New nonradioactive microspheres and more sensitive X-ray fluorescence to measure regional blood flow. Am J Physiol Heart Circ Physiol.1992;263:H1946–H1957.

18 Ogita H, Node K, Asanuma H, Sanada S, Takashima S, Asakura M. Amelioration of ischemia- and reperfusion-induced myocardial injury by the selective estrogen receptor modulator, raloxifene, in the canine heart. J Am Coll Cardiol. 2002;40:998–1005.

19 Zhang N, Komine-Kobayashi M, Tanaka R, Liu M, Mizuno Y, Urabe T. Edaravone reduces early accumulation of oxidative products and sequential inflammatory responses after transient focal ischemia in mice brain. Stroke. 2005;36:2220–2225.

20 Nimata M, Okabe TA, Hattori M, Yuan Z, Shioji K, Kishimoto C. MCI-186 (edaravone), a novel free radical scavenger, protects against acute autoimmune myocarditis in rats. Am J Physiol Heart Circ Physiol. 2005;289:H2514–H2518.

21 Szocs K. Endothelial dysfunction and reactive oxygen species production in ischemia/reperfusion and nitrate tolerance. Gen Physiol Biophys. 2004;23:265–269.

22 Jitsuiki D, Higashi Y, Goto C, Kimura M, Noma K, Hara K, et al. Effect of edaravone, a novel free radical scavenger, on

endothelium-dependent vasodilation in smokers. Am J Cardiol. 2004;94:1070–10703.

23 Neishi Y, Mochizuki S, Miyasaka T, Kawamoto T, Kume T, Sukmawan R, et al. Evaluation of bioavailability of nitric oxide in coronary circulation by direct measurement of plasma nitric oxide concentration. Proc Natl Acd Sci U S A. 2005;102:11456–11461.

24 Yada T, Shimokawa H, Hiramatsu O, Kajita T, Shigeto F, Goto M, et al. Hydrogen peroxide, an endogenous endothelium-derived hyperpolarizing factor, plays an important role in coronary autoregulation in vivo. Circulation. 2003;107:1040–1045.

25 Yoshida H, Sasaki K, Namiki Y, Sato N, Tada N. Edaravone, a novel radical scavenger, inhibits oxidative modification of low-density lipoprotein (LDL) and reverses oxidized LDL-mediated reduction in the expression of endothelial nitric oxide synthase. Atherosclerosis. 2005;179:97–102.

26 DeFily DV, Chilian WM. Preconditioning protects coronary arteriolar endothelium from ischemia-reperfusion injury. Am J Physiol. 1993;265:H700–H706.

27 Wu TW, Zeng LH, Wu J, Fung KP. Myocardial protection of MCI-186 in rabbit ischemia-reperfusion. Life Sci. 2002;71: 2249–2255.

Journal of the American College of Cardiology
© 2007 by the American College of Cardiology Foundation
Published by Elsevier Inc.

Vol. 50, No. 13, 2007
ISSN 0735-1097/07/$32.00
doi:10.1016/j.jacc.2007.05.039

PRECLINICAL STUDIES

Important Role of Endogenous Hydrogen Peroxide in Pacing-Induced Metabolic Coronary Vasodilation in Dogs In Vivo

Toyotaka Yada, MD, PHD,* Hiroaki Shimokawa, MD, PHD,† Osamu Hiramatsu, PHD,* Yoshiro Shinozaki, BS,‡ Hidezo Mori, MD, PHD,§ Masami Goto, MD, PHD,* Yasuo Ogasawara, PHD,* Fumihiko Kajiya, MD, PHD*

Kurashiki, Sendai, Isehara, and Suita, Japan

Objectives We examined whether endogenous hydrogen peroxide (H_2O_2) is involved in pacing-induced metabolic vasodilation in vivo.

Background We have previously demonstrated that endothelium-derived H_2O_2 is an endothelium-derived hyperpolarizing factor in canine coronary microcirculation in vivo. However, the role of endogenous H_2O_2 in metabolic coronary vasodilation in vivo remains to be examined.

Methods Canine subepicardial small coronary arteries (≥100 μm) and arterioles (<100 μm) were continuously observed by a microscope under cyclooxygenase blockade (ibuprofen, 12.5 mg/kg intravenous [IV]) (n = 60). Experiments were performed during paired right ventricular pacing under the following 7 conditions: control, nitric oxide (NO) synthase inhibitor (N^G-monomethyl-L-arginine [L-NMMA], 2 μmol/min for 20 min intracoronary [IC]), catalase (a decomposer of H_2O_2, 40,000 U/kg IV and 240,000 U/kg/min for 10 min IC), 8-sulfophenyltheophylline (SPT) (an adenosine receptor blocker, 25 μg/kg/min for 5 min IC), L-NMMA+catalase, L-NMMA+tetraethylammonium (TEA) (K_{Ca}-channel blocker, 10 μg/kg/min for 10 min IC), and L-NMMA+catalase+8-SPT.

Results Cardiac tachypacing (60 to 120 beats/min) caused coronary vasodilation in both-sized arteries under control conditions in response to the increase in myocardial oxygen consumption. The metabolic coronary vasodilation was decreased after L-NMMA in subepicardial small arteries with an increased fluorescent H_2O_2 production compared with catalase group, whereas catalase decreased the vasodilation of arterioles with an increased fluorescent NO production compared with the L-NMMA group, and 8-SPT also decreased the vasodilation of arterioles. Furthermore, the metabolic coronary vasodilation was markedly attenuated after L-NMMA+catalase, L-NMMA+TEA, and L-NMMA+catalase+8-SPT in both-sized arteries.

Conclusions These results indicate that endogenous H_2O_2 plays an important role in pacing-induced metabolic coronary vasodilation in vivo. (J Am Coll Cardiol 2007;50:1272–8) © 2007 by the American College of Cardiology Foundation

Cardiac tachycardia by pacing or exercise increases myocardial oxygen consumption (MVO_2) and increases coronary blood flow by several mechanisms (1–3). Shear stress plays a crucial role in modulating vascular tone by endothelium-derived releasing factors (EDRFs), including nitric oxide (NO), prostacyclin (PGI_2), and endothelium-derived hyperpolarizing factor (EDHF) (4,5). Flow-induced vasodilation is mediated by either NO (6,7), PGI_2 (8), both of them (9), or EDHF (10). Matoba et al. have previously identified that endothelium-derived hydrogen peroxide (H_2O_2) is a primary EDHF in mesenteric arteries of mice and humans (11,12). Morikawa et al. (13,14) subsequently confirmed

See page 1279

From the *Department of Medical Engineering and Systems Cardiology, Kawasaki Medical School, Kurashiki, Japan; †Department of Cardiovascular Medicine, Tohoku University Graduate School of Medicine, Sendai, Japan; ‡Department of Physiology, Tokai University School of Medicine, Isehara, Japan; and the §Department of Cardiac Physiology, National Cardiovascular Center Research Institute, Suita, Japan. Dr. Yada is the winner of the Endothelium-Derived Hyperpolarizing Factor (EDHF) Tanabe Award from the Scientific Sessions of the American Heart Association, November 2005, Dallas, Texas.

This work was supported in part by grants from the Japanese Ministry of Education, Science, Sports, Culture, and Technology, Tokyo, Japan, Nos. 16209027 (to Dr. Shimokawa) and 16300164 (to Dr. Yada), the Program for Promotion of Fundamental Studies in Health Sciences of the Organization for Pharmaceutical Safety and Research of Japan (to Dr. Shimokawa), and Takeda Science Foundation 2002 (to Dr. Yada).

Manuscript received September 11, 2006; revised manuscript received April 25, 2007, accepted May 1, 2007.

that endothelial Cu,Zn-superoxide dismutase (SOD) plays an important role as an EDHF synthase in mice and humans. Miura et al. (15) demonstrated that endothelium-derived H_2O_2 is involved as an EDHF in the flow-induced vasodilation of isolated human coronary arterioles in vitro. We have recently confirmed that endogenous H_2O_2 plays an important compensatory role during coronary autoregulation (16) and reperfusion injury in vivo (17) through the interactions with NO and adenosine.

It is known that vascular α-adrenergic receptor is modulated by the endothelium in dogs (18), whereas cardiac β-adrenergic receptor is modulated by K_{Ca} channels in pigs (19) and H_2O_2 in mice (20). However, the role of endogenous H_2O_2 in metabolic coronary vasodilation in vivo remains largely unknown. In the present study, we thus examined whether H_2O_2 is involved in pacing-induced metabolic coronary vasodilation in canine coronary microcirculation in vivo.

Abbreviations and Acronyms

CBF = coronary blood flow
DAR = diaminorhodamine-4M AM
DCF = 2′,7′-dichlorodihydrofluorescein diacetate
EDHF = endothelium-derived hyperpolarizing factor
H_2O_2 = hydrogen peroxide
L-NMMA = N^G-monomethyl-L-arginine
LAD = left anterior descending coronary artery
MVO_2 = myocardial oxygen consumption
NO = nitric oxide
PGI_2 = prostacyclin
SPT = sulfophenyltheophylline
TEA = tetraethylammonium

Methods

This study conformed to the Guideline on Animal Experiments of Kawasaki Medical School and the Guide for the Care and Use of Laboratory Animals published by the U.S. National Institutes of Health.

Animal preparation. Anesthetized mongrel dogs of either gender (15 to 25 kg in body weight, n = 60) were ventilated with a ventilator (Model VS600, IDC, Pittsburgh, Pennsylvania). We continuously monitored aortic pressure and left ventricular pressure (LVP) with a catheter (SPC-784A, Millar, Houston, Texas) and blood flow of the left anterior descending coronary artery (LAD) with a transonic flow probe (T206, Transonic Systems, Ithaca, New York).

Measurements of coronary diameter by intravital microscope. We continuously monitored coronary vascular responses by an intravital microscope (VMS 1210, Nihon Kohden, Tokyo, Japan) with a needle-probe in vivo, as previously described (21). We gently placed the needle-probe on subepicardial microvessels. When a clear vascular image was obtained, end-diastolic vascular images were taken with 30 pictures/s (21).

Measurements of regional myocardial blood flow. Regional myocardial blood flow was measured by the nonradioactive microsphere (Sekisui Plastic Co. Ltd., Tokyo, Japan) technique, as previously described (22). Briefly, the microspheres suspension was injected into the left atrium 3 min after tachypacing. Myocardial flow in the LAD area was calculated according to the formula "time flow = tissue counts × (reference flow/reference counts)" and was expressed in ml/g/min (22).

Detection of H_2O_2 and NO production in coronary microvessels. 2′,7′-dichlorodihydrofluorescein diacetate (DCF) (Molecular Probes, Eugene, Oregon) and diaminorhodamine-4M AM (DAR) (Daiichi Pure Chemicals, Tokyo, Japan) were used to detect H_2O_2 and NO production in coronary microvessels, respectively, as previously described (17). Briefly, fresh and unfixed heart tissues were cut into several blocks and immediately frozen in optimal cutting temperature compound (Tissue-Tek, Sakura Fine Chemical, Tokyo, Japan). Fluorescent images of the microvessels were obtained 3 min after application of acetylcholine (ACh) by using a fluorescence microscope (OLYMPUS BX51, Tokyo, Japan) (17).

Experimental protocols. After the surgical procedure and instrumentation, at least 30 min were allowed for stabilization while monitoring hemodynamic variables. Coronary vasodilator responses were examined before and after cardiac tachypacing (60 to 120 beats/min) under the following 7 conditions with cyclooxygenase blockade (ibuprofen, 12.5 mg/kg, IV) to evaluate the role of H_2O_2 and NO without PGI_2 in a different set of animals (Fig. 1): 1) control conditions without any inhibitor; 2) L-NMMA alone (2 μmol/min intracoronary [IC] for 20 min); 3) catalase alone (40,000 U/kg intravenous [IV] and 240,000 U/kg/min IC for 10 min, an enzyme that dismutates

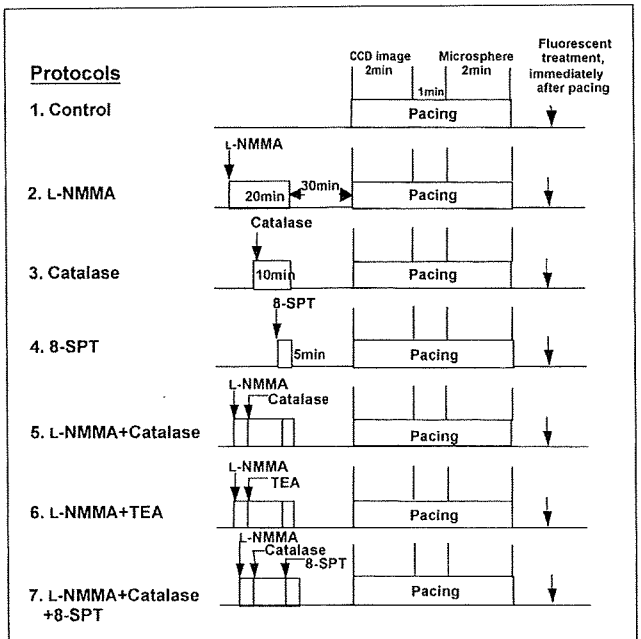

Figure 1 Experimental Protocols

CCD = charge-coupled device; L-NMMA = N^G-monomethyl-L-arginine; SPT = sulfophenyltheophylline; TEA = tetraethylammonium.

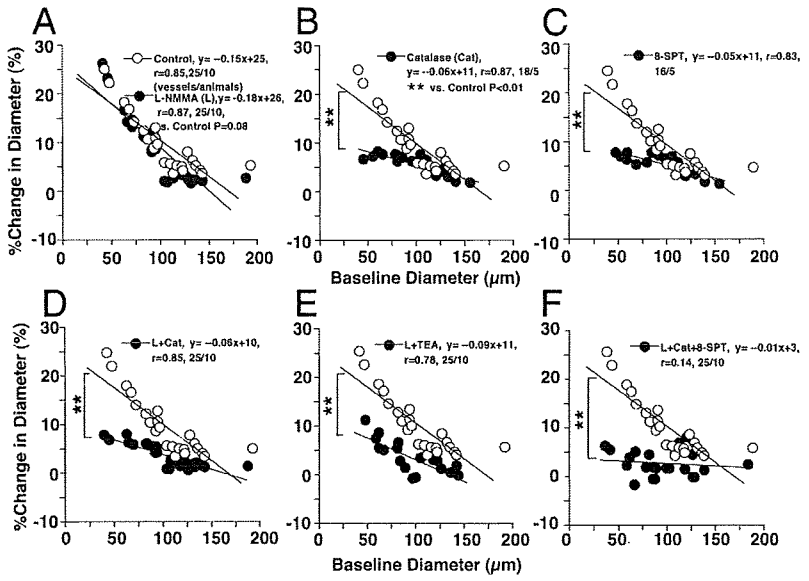

Figure 2 Coronary Vascular Responses to Cardiac Pacing

The coronary vasodilating responses of both-sized coronary arteries were significantly inhibited in all experimental conditions except L-NMMA alone. **p < 0.01. Abbreviations as in Figure 1.

H_2O_2 into water and oxygen); 4) adenosine receptor blockade alone (8-sulfophenyltheophylline [8-SPT], 25 μg/kg/min IC for 5 min); 5) catalase plus L-NMMA; 6) catalase plus tetraethylammonium (TEA) (10 μg/kg/min IC for 10 min, an inhibitor of large conductance K_{Ca} channels to inhibit EDHF-mediated responses) (23); and 7) catalase plus L-NMMA with 8-SPT (16). These inhibitors were given at 30 min before cardiac tachypacing (Fig. 1). The basal coronary diameter was defined as that before pacing. We continuously observed the diameter change in subepicardial small coronary arteries (≥100 μm) and arterioles (<100 μm) with an intravital microscope before and at 2 min after pacing. Microspheres were administered at 3 min after the pacing was started (Fig. 1). In the combined infusion protocol (L-NMMA+catalase+8-SPT), L-NMMA infusion was first started, followed by catalase infusion, and then 8-SPT was added at 15 min after the initiation of L-NMMA infusion (Fig. 1). Then, fresh and unfixed heart tissues were cut into several blocks and immediately frozen in optimal cutting temperature compound after the pacing. The flow and MVO_2 were measured as full-thickness values.

Drugs. All drugs were obtained from Sigma Chemical Co. and were diluted in a physiological saline immediately before use.

Statistical analysis. Results are expressed as means ± SEM. Differences in the vasodilation of subepicardial coronary microvessels before and after pacing (Fig. 2) were examined by a multiple regression analysis using a model, in which the change in coronary diameter was set as a dependent variable (y) and vascular size as an explanatory variable (x), while the statuses of control and other inhibitors were set as dummy variables (D1, D2) in the following equation: $y = a0 + a1x + a2D1 + a3D2$, where a0 through a3 are partial regression coefficients (16). Significance tests were made as simultaneous tests for slope and intercept differences. Pairwise comparisons against control were made without adjustment for multiple comparisons. The vessel was the unit of analysis without correction for correlated observations. The power of this analysis is greater than that of using the animal as the unit of analysis, giving smaller p values. Vascular fluorescent responses (Figs. 3 and 4) were analyzed by one-way analysis of variance followed by Scheffe's post hoc test for multiple comparisons. The criterion for statistical significance was at $p < 0.05$.

Results

Hemodynamic status and blood gases during pacing. Throughout the experiments, mean aortic pressure was constant and comparable (Table 1), and pO_2, pCO_2, and pH were maintained within the physiological ranges (pO_2 >70 mm Hg, pCO_2 25 to 40 mm Hg, and pH 7.35 to 7.45). Baseline coronary diameter was comparable in the absence and presence of inhibitors under the 7 different experimental conditions (Table 1). Cardiac tachypacing increased coronary blood flow and MVO_2 from the baseline values (Table 2, both $p < 0.01$). Combined infusion of L-NMMA+catalase+8-SPT significantly decreased coronary blood flow (CBF) and MVO_2 as compared with control, L-NMMA alone (both $p < 0.01$), catalase alone (both $p < 0.01$), 8-SPT alone (both $p < 0.01$), L-NMMA+catalase (both $p < 0.05$), L-NMMA+TEA (both $p < 0.05$). Com-

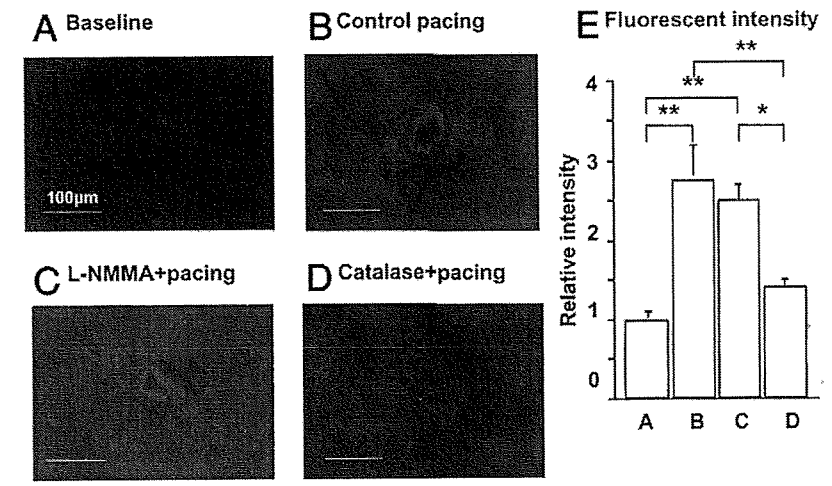

Figure 3 Detection of H_2O_2 Production With DCF Fluorescent Method

Hydrogen peroxide (H_2O_2) production was unaltered after N^G-monomethyl-L-arginine (L-NMMA) but was markedly suppressed by catalase. Number of arterioles/animals used was 5/5 for each group. *$p < 0.05$, **$p < 0.01$. DCF = 2′,7′-dichlorodihydrofluorescein diacetate.

bined infusion of L-NMMA+catalase or L-NMMA+TEA significantly decreased CBF (both $p < 0.05$) and MVO_2 (both $p < 0.05$) as compared with control after the pacing.

Coronary vasodilation before and after cardiac tachypacing. Cardiac tachypacing caused coronary vasodilation in both-sized arteries under control conditions (small coronary arteries, 5 ± 1%; arterioles, 14 ± 2%) (Fig. 2A) with decreased coronary venous pO_2 (Table 2). The metabolic coronary vasodilation was significantly decreased after L-NMMA in small coronary arteries (3 ± 1%) but not in arterioles (14 ± 2%), whereas catalase and 8-SPT decreased the vasodilation of arterioles (both 4 ± 1%) but not in small coronary arteries (both 7 ± 1%) (Figs. 2B and 2C). Furthermore, the metabolic coronary vasodilation was markedly attenuated after L-NMMA+catalase and L-NMMA+TEA in small coronary arteries (both 2 ± 1%), and L-NMMA+catalase+8-SPT almost abolished the vasodilating responses in both-sized arteries (small coronary arteries, −1 ± 1%; arterioles, 1 ± 1%) (Figs. 2D to 2F). When expressed in a linear regression analysis, the coronary vasodilating responses of both-sized coronary arteries were significantly inhibited in all experimental conditions except L-NMMA alone (Fig. 2A).

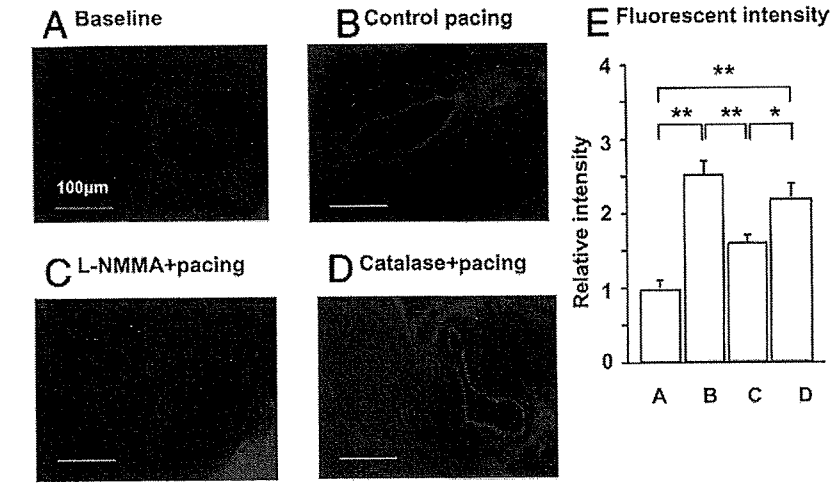

Figure 4 Detection of NO Production With DAR Fluorescent Method

Nitric oxide (NO) production was unaltered after catalase but was markedly suppressed by N^G-monomethyl-L-arginine (L-NMMA). Number of arterioles/animals used was 5/5 for each group. *$p < 0.05$, **$p < 0.01$. DAR = diaminorhodamine-4M AM.

Table 1 The Small Artery and Arteriolar Diameter Measurements at Rest and During Cardiac Pacing

	Control	L-NMMA (L)	Catalase (Cat)	8-SPT	L+Cat	L+TEA	L+Cat+8-SPT
Small artery							
n (vessels/dogs)	12/10	12/10	9/5	7/5	12/10	12/10	12/10
Rest (μm)	127 ± 7	125 ± 6	127 ± 5	126 ± 6	125 ± 7	123 ± 6	124 ± 7
Cardiac pacing (μm)	134 ± 7*	129 ± 7†	132 ± 5*	131 ± 6*	127 ± 7	124 ± 6	123 ± 6
Arteriole							
n (vessels/dogs)	12/10	12/10	9/5	9/5	12/10	12/10	12/10
Rest (μm)	75 ± 5	73 ± 5	71 ± 5	71 ± 5	72 ± 5	74 ± 5	72 ± 6
Cardiac pacing (μm)	85 ± 5*	82 ± 5*	77 ± 6†	77 ± 6†	77 ± 5†	77 ± 5	73 ± 5

Results are expressed as mean ± SEM. *$p < 0.01$, †$p < 0.05$ versus rest.
L-NMMA = N^G-monomethyl-L-arginine; SPT = sulfophenyltheophylline; TEA = tetraethylammonium.

Detection of H_2O_2 and NO production. Fluorescent microscopy with DCF showed that cardiac tachypacing increased coronary H_2O_2 production compared with baseline conditions in arterioles (Fig. 3). The pacing-induced H_2O_2 production as assessed by DCF fluorescent intensity was unaltered after L-NMMA but was markedly suppressed by catalase (Fig. 3). By contrast, in small coronary arteries, vascular NO production as assessed by DAR fluorescent intensity was significantly increased in response to the pacing compared with baseline conditions (Fig. 4). The pacing-induced NO production was unaltered after catalase but was markedly suppressed by L-NMMA (Fig. 4). Pacing caused no significant increase in H_2O_2 production in small coronary arteries or NO production in arterioles (data not shown).

Discussion

The major finding of the present study is that endogenous H_2O_2 plays an important role in pacing-induced metabolic coronary dilation as a compensatory mechanism for NO in vivo. We demonstrated the important role of endogenous H_2O_2 in the mechanisms for metabolic coronary dilation in vivo.

Validations of experimental model and methodology. We chose, on the basis of our previous reports (16,17), the adequate dose of L-NMMA, catalase, TEA, and 8-SPT in order to inhibit NO synthesis, H_2O_2, K_{Ca} channels, and the adenosine receptor, respectively. The TEA at low doses is fairly specific for K_{Ca} channel, but at higher doses it might block a number of other K channels. Because several K_{Ca} channels might be involved in H_2O_2-mediated responses (5), we selected nonselective K_{Ca} inhibitor, TEA, to inhibit all K_{Ca} channels (23). We have previously confirmed the validity of our present methods (21).

Role of NO and H_2O_2 after cardiac pacing. Matoba et al. have demonstrated that endothelium-derived H_2O_2 is an EDHF in mouse (11) and human (12) mesenteric arteries and pig coronary microvessels (24). Morikawa et al. also

Table 2 Hemodynamic Status at Rest and During Cardiac Pacing

	Control	L-NMMA (L)	Catalase (Cat)	8-SPT	L+Cat	L+TEA	L+Cat+8-SPT
n (dogs)	10	10	5	5	10	10	10
SBP							
Rest (mm Hg)	135 ± 14	135 ± 14	114 ± 9	123 ± 5	98 ± 9	99 ± 9	96 ± 8
Cardiac pacing	137 ± 14	136 ± 14	125 ± 12	130 ± 7	100 ± 9	100 ± 8	103 ± 9
MBP							
Rest (mm Hg)	117 ± 10	117 ± 10	98 ± 8	99 ± 5	89 ± 10	90 ± 10	87 ± 9
Cardiac pacing	124 ± 9	120 ± 13	107 ± 10	110 ± 7	91 ± 10	92 ± 10	92 ± 10
DP							
Rest	8,100 ± 845	8,100 ± 845	6,855 ± 527	7,350 ± 312	5,880 ± 537	5,910 ± 527	5,730 ± 478
Cardiac pacing	16,440 ± 1,718*	16,320 ± 1,680*	15,000 ± 1,423*	15,630 ± 778*	11,940 ± 11,029*	12,000 ± 1,011*	12,300 ± 1,078*
$CVPO_2$							
Rest (mm Hg)	20 ± 1	17 ± 1	16 ± 1	17 ± 1	15 ± 1†	15 ± 1†	14 ± 1†
Cardiac pacing	14 ± 1*	11 ± 1*	11 ± 1*	12 ± 1*	10 ± 1*†	10 ± 1*†	9 ± 1*†
MVO_2							
Rest (μlO_2/min/g)	70 ± 2	66 ± 2	67 ± 2	73 ± 5	62 ± 5	61 ± 5	60 ± 5
Cardiac pacing	171 ± 4‡	168 ± 2‡	158 ± 12‡	168 ± 13‡	133 ± 4†‡	130 ± 18†‡	95 ± 9*§
CBF							
Rest (ml/min/g)	0.66 ± 0.06	0.63 ± 0.06	0.66 ± 0.03	0.66 ± 0.01	0.59 ± 0.06	0.62 ± 0.05	0.51 ± 0.04
Cardiac pacing	1.48 ± 0.32‡	1.46 ± 0.06‡	1.36 ± 0.02‡	1.40 ± 0.01‡	1.22 ± 0.01†‡	1.24 ± 0.12†‡	0.96 ± 0.07‡§

Results are expressed as mean ± SEM. *$p < 0.05$ versus at rest. †$p < 0.05$ versus corresponding control measurements. ‡$p < 0.01$ versus rest. §$p < 0.01$ versus corresponding control measurements.
CBF = coronary blood flow; $CVPO_2$ = coronary venous pO_2; DP = double product; MBP = mean blood pressure; MVO_2 = myocardial oxygen consumption; SBP = systolic blood pressure; other abbreviations as in Table 2.

have demonstrated that endothelial Cu,Zn-SOD plays an important role as an H_2O_2/EDHF synthase in mouse (13) and human (14) mesenteric arteries. Subsequently, we (16,17) and others (15) confirmed that endogenous H_2O_2 exerts important vasodilator effects in canine coronary microcirculation in vivo and in isolated human coronary microvessels, respectively. In the present study, the pacing-induced metabolic coronary vasodilation was significantly decreased after L-NMMA in small coronary arteries but not in arterioles, whereas catalase decreased the vasodilation of arterioles but not that of small arteries, and the coronary vasodilation was markedly attenuated after L-NMMA+catalase (Fig. 2). These findings indicate that NO and H_2O_2 compensate for each other to maintain coronary vasodilation in response to increased myocardial oxygen demand. Coronary venous pO_2 tended to be lower after L-NMMA+catalase, suggesting that NO and H_2O_2 coordinately cause coronary vasodilation during cardiac tachypacing.

Saitoh et al. (25) suggested that the production of H_2O_2, which stems from the dismutation of $\cdot O_2^-$ that is formed during mitochondrial electron transport, is seminal in the coupling between oxygen metabolism and blood flow in the heart. Thus, the contribution of H_2O_2 production in response to the change in metabolism cannot be excluded.

Endothelial Cu,Zn-SOD plays an important role in the synthesis of H_2O_2 as an EDHF synthase in mouse (13) and human (14) mesenteric arteries, and exercise training enhances expression of Cu,Zn-SOD in normal pigs (26). It remains to be examined whether exercise-induced upregulation of Cu,Zn-SOD enhances metabolic coronary vasodilation mediated by endogenous H_2O_2.

Compensatory vasodilator mechanism among H_2O_2, NO, and adenosine. The EDHF acts as a partial compensatory mechanism to maintain endothelium-dependent vasodilation in the forearm microcirculation of patients with essential hypertension, where NO activity is impaired owing to oxidative stress (27). We have recently demonstrated in the fluorescent microscopy study that coronary vascular production of H_2O_2 and NO is enhanced after myocardial ischemia/reperfusion in small coronary arteries and arterioles, respectively (17). In the present study, the DCF fluorescent intensity was comparable between control and L-NMMA, and that of DAR was also comparable between control and catalase (Figs. 3 and 4). Although the exact source of vascular production of H_2O_2 and NO remains to be elucidated, it is highly possible that endothelium-derived NO and H_2O_2 compensate for each other to maintain coronary vasodilation in response to increased MVO_2.

In the dog, blockade of any vasodilator mechanisms fails to blunt the increase in coronary blood flow in response to exercise, indicating that adenosine, K^+_{ATP}-channel opening, prostanoids, or NO might not be mandatory for exercise-induced coronary vasodilation, or that these redundant vasodilator mechanisms compensate for each other when one mechanism is blocked (28). In the present study, adenosine blockade with 8-SPT alone inhibited the pacing-induced vasodilation of arteriole but not that of small artery, whereas combined administration of L-NMMA+catalase+8-SPT almost abolished the pacing-induced coronary vasodilation of both-sized arteries with an increase in coronary blood flow (Fig. 2). The discrepancy between the diameter and flow responses is likely due to the metabolic autoregulation of smaller arterioles. These results indicate that adenosine also plays an important role to maintain metabolic coronary vasodilation in cooperation with NO and H_2O_2, a finding consistent with our previous study on coronary autoregulatory mechanisms (15).

Study limitations. Several limitations should be mentioned for the present study. First, although we were able to demonstrate the production of H_2O_2 with fluorescent microscopy with DCF, we were unable to quantify the endothelial H_2O_2 production, because DCF reacts with H_2O_2, peroxynitrite, and hypochlorous acid (13). Second, we were unable to find smaller arterioles, owing to the limited spatial resolution of our charge-coupled device intravital microscope. With an intravital camera with higher resolution, we would be able to observe coronary vasodilation of smaller arterioles. Third, we were unable to determine whether H_2O_2 is produced by shear stress or cardiac metabolism. This point remains to be elucidated in a future study.

Conclusions

We were able to demonstrate that endogenous H_2O_2 plays an important role in pacing-induced metabolic coronary vasodilation in canine coronary microcirculation in vivo and that there are substantial compensatory interactions among NO, H_2O_2, and adenosine to maintain metabolic coronary vasodilation, which is one of the most important mechanisms for cardiovascular homeostasis in vivo.

Reprint requests and correspondence: Dr. Toyotaka Yada, Department of Medical Engineering and Systems Cardiology, Kawasaki Medical School, 577 Matsushima, Kurashiki, Okayama 701-0192, Japan. E-mail: yada@me.kawasaki-m.ac.jp.

REFERENCES

1. Ishibashi Y, Duncker DJ, Zhang J, Bache RJ. ATP-sensitive K^+ channels, adenosine, and nitric oxide-mediated mechanisms account for coronary vasodilation during exercise. Circ Res 1998;82:346–59.
2. Jones CJ, Kuo L, Davis MJ, DeFily DV, Chilian WM. Role of nitric oxide in the coronary microvascular responses to adenosine and increased metabolic demand. Circulation 1995;91:1807–13.
3. Yada T, Richmond KN, Van Bibber R, Kroll K, Feigl EO. Role of adenosine in local metabolic coronary vasodilation. Am J Physiol 1999;276:H1425–33.
4. Feletou M, Vanhoutte PM. Endothelium-dependent hyperpolarization of canine smooth muscle. Br J Pharmacol 1988;93:515–24.
5. Shimokawa H. Primary endothelial dysfunction: atherosclerosis. J Mol Cell Cardiol 1999;31:23–37.
6. Kuo L, Davis MJ, Chilian WM. Endothelium-dependent, flow-induced dilation of isolated coronary arterioles. Am J Physiol 1991; 259:H1063–70.

7. Kuo L, Chilian WM, Davis MJ. Interaction of pressure- and flow-induced responses in porcine coronary resistance vessels. Am J Physiol 1991;261:H1706–15.
8. Koller A, Sun D, Kaley G. Role of shear stress and endothelial prostaglandins in flow- and viscosity-induced dilation of arterioles in vitro. Circ Res 1993;72:1276–84.
9. Koller A, Sun D, Huang A, Kaley G. Corelease of nitric oxide and prostaglandins mediates flow-dependent dilation of ratgracilis muscle arterioles. Am J Physiol 1994;267:H326–32.
10. Takamura Y, Shimokawa H, Zhao H, et al. Important role of endothelium-derived hyperpolarizing factor in shear stress-induced endothelium-dependent relaxations in the rat mesenteric artery. J Cardiovasc Pharmacol 1999;34:381–7.
11. Matoba T, Shimokawa H, Nakashima M, et al. Hydrogen peroxide is an endothelium-derived hyperpolarizing factor in mice. J Clin Invest 2000;106:1521–30.
12. Matoba T, Shimokawa H, Kubota H, et al. Hydrogen peroxide is an endothelium-derived hyperpolarizing factor in human mesenteric arteries. Biochem Biophys Res Comm 2002;290:909–13.
13. Morikawa K, Shimokawa H, Matoba T, et al. Pivotal role of Cu,Zn-superoxide dismutase in endothelium-dependent hyperpolarization. J Clin Invest 2003;112:1871–9.
14. Morikawa K, Fujiki T, Matoba T, et al. Important role of superoxide dismutase in EDHF-mediated responses of human mesenteric arteries. J Cardiovasc Pharmacol 2004;44:552–6.
15. Miura H, Bosnjak JJ, Ning G, Saito T, Miura M, Gutterman DD. Role for hydrogen peroxide in flow-induced dilation of human coronary arterioles. Circ Res 2003;92:e31–40.
16. Yada T, Shimokawa H, Hiramatsu O, et al. Hydrogen peroxide, an endogenous endothelium-derived hyperpolarizing factor, plays an important role in coronary autoregulation in vivo. Circulation 2003; 107:1040–5.
17. Yada T, Shimokawa H, Hiramatsu O, et al. Cardioprotective role of endogenous hydrogen peroxide during ischemia-reperfusion injury in canine coronary microcirculation in vivo. Am J Physiol 2006;291: H1138–46.
18. Jones CJ, DeFily DV, Patterson JL, Chilian WM. Endothelium-dependent relaxation competes with alpha 1- and alpha 2-adrenergic constriction in the canine epicardial coronary microcirculation. Circulation 1993;87:1264–74.
19. Scornik FS, Codina J, Birnbaumer L, Toro L. Modulation of coronary smooth muscle K_{Ca} channels by Gs alpha independent of phosphorylation by protein kinase A. Am J Physiol 1993;265:H1460–5.
20. Tan CM, Xenoyannis S, Feldman RD. Oxidant stress enhances adenylyl cyclase activation. Circ Res 1995;77:710–7.
21. Yada T, Hiramatsu O, Kimura A, et al. In vivo observation of subendocardial microvessels of the beating porcine heart using a needle-probe videomicroscope with a CCD camera. Circ Res 1993; 72:939–46.
22. Mori H, Haruyama Y, Shinozaki H, et al. New nonradioactive microspheres and more sensitive X-ray fluorescence to measure regional blood flow. Am J Physiol 1992;263:H1946–57.
23. Masumoto A, Hirooka Y, Shimokawa H, Hironaga K, Setoguchi S, Takeshita A. Possible involvement of Rho-kinase in the pathogenesis of hypertension in humans. Hypertension 2001;38:1307–10.
24. Matoba T, Shimokawa H, Morikawa K, et al. Electron spin resonance detection of hydrogen peroxide as an endothelium-derived hyperpolarizing factor in porcine coronary microvessels. Arterioscler Thromb Vasc Biol 2003;23:1224–30.
25. Saitoh S, Zhang C, Tune JD, et al. Hydrogen peroxide: a feed-forward dilator that couples myocardial metabolism to coronary blood flow. Arterioscler Thromb Vasc Biol 2006;26:2614–21.
26. Rush JW, Laughlin MH, Woodman CR, Price EM. SOD-1 expression in pig coronary arterioles is increased by exercise training. Am J Physiol 2000;279:H2068–76.
27. Taddei S, Versari D, Cipriano A, et al. Identification of a cytochrome P450 2C9-derived endothelium- derived hyperpolarizing factor in essential hypertensive patients. J Am Coll Cardiol 2006;48:508–15.
28. Duncker DJ, Bache RJ. Regulation of coronary vasomotor tone under normal conditions and during acute myocardial hypoperfusion. Pharmacol Ther 2000;86:87–110.

Acta Physiol 2007, 191, 275–284

Characterization of ouabain-induced noradrenaline and acetylcholine release from *in situ* cardiac autonomic nerve endings

T. Yamazaki,[1] T. Akiyama,[1] H. Kitagawa,[1] F. Komaki,[1] H. Mori,[1] T. Kawada,[2] K. Sunagawa[2] and M. Sugimachi[2]

1 Department of Cardiac Physiology, National Cardiovascular Center Research Institute, Suita, Osaka, Japan

2 Department of Cardiovascular Dynamics, National Cardiovascular Center Research Institute, Suita, Osaka, Japan

Received 11 January 2007, revision requested 28 March 2007, revision received 29 May 2007, accepted 30 June 2007
Correspondence: T. Yamazaki, Department of Cardiac Physiology, National Cardiovascular Center Research Institute, 5-7-1 Fujishirodai, Suita, Osaka 565, Japan. E-mail: yamazaki@ri.ncvc.go.jp

Abstract

Aim: Although ouabain modulates autonomic nerve ending function, it is uncertain whether ouabain-induced releasing mechanism differs between *in vivo* sympathetic and parasympathetic nerve endings. Using cardiac dialysis, we examined how ouabain induces neurotransmitter release from autonomic nerve ending.

Methods: Dialysis probe was implanted in left ventricle, and dialysate noradrenaline (NA) or acetylcholine (ACh) levels in the anaesthetized cats were measured as indices of neurotransmitter release from post-ganglionic autonomic nerve endings.

Results: Locally applied ouabain (100 μM) increased in dialysate NA or ACh levels. The ouabain-induced increases in NA levels remained unaffected by cardiac sympathetic denervation and tetrodotoxin (Na^+ channel blocker, TTX), but the ouabain-induced increases in ACh levels were attenuated by TTX. The ouabain-induced increases in NA levels were suppressed by pretreatment with desipramine (NA transport blocker) and augmented by reserpine (vesicle NA transport blocker). In contrast, the ouabain-induced increases in ACh levels remained unaffected by pretreatment with hemicholinium-3 (choline transport blocker) but suppressed by vesamicol (vesicle ACh transport blocker). The ouabain-induced increases in NA levels were suppressed by pretreatment with ω-conotoxin GVIA (N-type Ca^{2+} channel blocker), verapamil (L-type Ca^{2+} channel blocker) and TMB-8 (intracellular Ca^{2+} antagonist). The ouabain-induced increases in ACh levels were suppressed by pretreatment with ω-conotoxin MVIIC (P/Q-type Ca^{2+} channel blocker), and TMB-8.

Conclusions: Ouabain-induced NA release is attributable to the mechanisms of regional exocytosis and/or carrier-mediated outward transport of NA, from stored NA vesicle and/or axoplasma, respectively, while the ouabain-induced ACh release is attributable to the mechanism of exocytosis, which is triggered by regional depolarization. At both sympathetic and parasympathetic nerve endings, the regional exocytosis is because of opening of calcium channels and intracellular calcium mobilization.

Keywords acetylcholine, Ca^{2+} channels, cat, microdialysis, Na^+,K^+-ATPase, noradrenaline.

 doi: 10.1111/j.1748-1716.2007.01749.x

It is generally accepted that ouabain modulates autonomic nerve function by inhibition of membrane Na^+,K^+-ATPase (Gillis & Quest 1979). This neuronal modulatory effect was mainly reported with *in vitro* sympathetic (Sweadner 1985), parasympathetic nerve endings (Satoh & Nakazato 1992, Gomez *et al.* 1996) and adrenal glands (Haass *et al.* 1997). Furthermore, ouabain-induced modulatory effect was reported with *in vitro* studies on motor endplate (Vyskocil & Illes 1977, Zemkova *et al.* 1990). From these *in vitro* studies, several mechanisms are presently suggested to induce release of neurotransmitter from the nerve endings. However, it is uncertain whether the manner of modulation differs between *in vivo* sympathetic and parasympathetic nerve endings. A major concern is whether ouabain induces a brisk increase in neurotransmitter efflux (spontaneous neurotransmitter release). Kranzhöfer *et al.* (1991) reported that ouabain-induced spontaneous noradrenaline (NA) release from sympathetic nerve endings. On the other hand, ouabain-induced spontaneous acetylcholine (ACh) release was reported *in vitro* studies using synaptosomes (Satoh & Nakazato 1992). No reports have described *in vivo* spontaneous ACh release evoked by ouabain. Further, a second issue is at which site ouabain induces neurotransmitter release: stored vesicle or axoplasma (Haass *et al.* 1997). NA and ACh release have been reported in stored vesicles and/or the axoplasma. It is uncertain, however, which site induces the predominant neurotransmitter release evoked by ouabain *in vivo*. Furthermore, the mechanisms underlying the neurotransmitter release evoked by ouabain remain unclear. Neuronal effects of ouabain have been attributed to the inhibitory action upon Na^+,K^+-ATPase and transmembrane sodium pump (Haass *et al.* 1997). As a consequence of the reduced sodium gradient at the plasma membrane, two possible mechanisms have been proposed to induce NA release from nerve endings; (i) carrier-mediated reversed NA transport, and (ii) Ca^{2+}-dependent exocytotic NA release. The manner and mechanisms of NA efflux have been extensively studied and accepted *in vivo* in isolated tissues (Sweadner 1985, Haass *et al.* 1997). However, it remains unclear whether these assumptions are valid in the cardiac sympathetic or parasympathetic nerve endings *in vivo*.

Cardiac dialysis technique in combination with highly sensitive measurement of NA or ACh has offered a powerful method for detecting the low level of dialysate NA or ACh obtained from the myocardial space (Akiyama *et al.* 1991, 1994). We demonstrated that dialysate NA or ACh levels were affected by local administration of pharmacological agents through dialysis probes, indicating that changes in dialysate NA or ACh levels reflect NA or ACh output from cardiac postganglionic sympathetic or parasympathetic nerve endings (Yamazaki *et al.* 1997, Kawada *et al.* 2001) respectively. Using dialysis technique, ouabain can be administered locally and it is possible to monitor NA or ACh output following locally applied ouabain (Yamazaki *et al.* 2001). Furthermore, comparison of the dialysate NA response in the presence and absence of neuronal agents can differentiate carrier-mediated NA release from calcium dependent exocytotic NA release (Yamazaki *et al.* 1997). With locally applied neuronal blockers, we examined the mechanisms and the sites underlying NA or ACh release evoked by ouabain.

Methods

Animal preparation

Adult cats were anaesthetized with pentobarbital sodium (30–35 mg kg^{-1} i.p.). The level of anaesthesia was maintained with a continuous intravenous infusion of pentobarbital sodium (1–2 mg kg^{-1} h^{-1}). The animals were intubated and ventilated with room air mixed with oxygen. Body temperature was maintained using a heated pad and lamp. All protocols were performed in accordance with the National Cardiovascular Center Research Institute Animal Care Ethics Committee guidelines that were in strict compliance with the NIH Guide for the Care and Use of Laboratory Animals. Electrocardiogram and mean arterial pressure were simultaneously monitored with a data recorder. The sixth rib on the left side was resected to expose the heart. With a fine guiding needle, one or two dialysis probes for dialysate sampling were implanted in the mid wall of the anterolateral region of the left ventricle. Heparin (100 U kg^{-1}) was administered after implantation of the dialysis probe and a maintenance dose was given every hour thereafter.

Dialysis technique

The material and properties of the dialysis probe were described previously (Akiyama *et al.* 1991, 1994). Briefly, we designed a transverse dialysis probe. Both ends of a dialysis fibre (13 mm length, 0.31 mm o.d. and 0.2 mm i.d.; PAN-1200, 50 000 molecular weight cutoff, Asahi Chemical, Tokyo, Japan) were connected and glued to polyethylene tubes (25 cm length, 0.5 mm o.d. and 0.2 mm i.d.). The dialysate NA or ACh levels were measured in separate animals. For the measurement of dialysate NA, the dialysis probe was perfused with Ringer's solution at 10 μL min^{-1}. Sampling periods were 2 min in duration (one sample volume = 20 μL), which was the minimum period necessary to collect sufficient NA for satisfactory measurement. For the measurement of dialysate ACh, Ringer's solution containing eserine (choline esterase

Journal compilation © 2007 Scandinavian Physiological Society, doi: 10.1111/j.1748-1716.2007.01749.x

inhibitor, 100 μM) was perfused at 2 μL min^{-1} and sampling periods were 15 min in duration. Dialysate sampling was started 120 min after probe implantation, when the dialysate NA or ACh concentration had reached a steady level. Each sample was collected in a microtube containing 0.1 N HCl or phosphate buffer to prevent oxidation. The dead-space volume between the dialysis and sample tube was measured. Taking this dead-space into account, samples were obtained.

Experimental protocols

In our previous study, we demonstrated that the dialysate NA or ACh levels reflect cardiac neuronal NA or ACh disposition at the nerve endings (Yamazaki *et al.* 1997, Kawada *et al.* 2001). Therefore, in the present study, we obtained dialysate samples and measured the dialysate NA or ACh levels as an index of NA or ACh output from post-ganglionic sympathetic or parasympathetic nerve endings respectively. Generally two mechanisms and sites are proposed to induce NA and ACh release from nerve endings: exocytotic (quantum) release from the stored vesicle and non-exocytotic (non-quantum) release from the axoplasma. The present studies were designed to clarify whether ouabain-induced NA or ACh efflux are affected by local administration of pharmacological agents that modify experimental conditions.

Protocol 1: Time courses of dialysate NA and ACh levels during local administration of ouabain. We examined the time course of dialysate NA and ACh levels during local administration of ouabain (100 μM). Ouabain was administered for 60 min. Dialysate NA levels were measured before and at 10-min intervals during ouabain administration. Dialysate ACh levels were collected in consecutive 15-min sampling periods.

Protocol 2: Influence of nerve transection and Na^+ channels on dialysate NA or ACh response evoked by ouabain. To test whether ouabain modulated central-mediated exocytotic neurotransmitter release, we examined the time course of ouabain-induced dialysate NA and ACh levels after transection of stellate ganglia or cervical parasympathetic nerve tract. For cardiac sympathetic denervation, the region of the stellate ganglia was exposed through the intercostal space, and bilateral transection of stellate ganglia was performed. After cardiac sympathetic denervation, heart rate response to carotid occlusion was blunted. In separate cats, cervical vagotomy was performed. We started dialysate sampling at 120 min after surgical interruption and ouabain-induced NA or ACh efflux was examined. Furthermore, to examine involvement of deporalization on NA or ACh release, ouabain-induced NA or ACh efflux was measured with addition of tetrodotoxin (TTX, 10 μM) through the dialysis probe. At 60 min after the beginning of TTX administration, we started the control sampling and examined the ouabain-induced NA or ACh response.

Protocol 3: Influence of NA-, ACh- and choline transporters on dialysate NA or ACh response evoked by ouabain. To test whether ouabain-induced neurotransmitter efflux was derived from axoplasma or stored vesicle, ouabain-induced NA or ACh efflux was examined with local administration of pharmacological agents, which affected the transport and content of neurotransmitter at the nerve endings. Membrane carrier-mediated NA transport was blocked by local administration of desipramine, whereas vesicular NA import was blocked by local administration of reserpine. In either case, ouabain-induced NA efflux was examined with the addition of desipramine (100 μM) or reserpine (10 μM) through the dialysis probe. The dosage of agent-administration was decided after referring to the previous studies (Akiyama *et al.* 1994, Yamazaki *et al.* 1997). Membrane carrier-mediated choline transport was blocked by local administration of hemicholinium-3 (10 μM), whereas vesicular ACh import was blocked by local administration of vesamicol (10 μM) (Kawada *et al.* 2001). In either case, ouabain-induced ACh efflux was examined with the addition of hemicholinium-3 or vesamicol through the dialysis probe.

Protocol 4: Influence of Ca^{2+} transporter, channel, mobilization on dialysate NA or ACh response evoked by ouabain. To test the contention that ouabain-induced neurotransmitter efflux was modulated by changes in intracellular Ca^{2+} levels, the influence of Ca^{2+} transporter, channel, mobilization on the dialysate NA or ACh response evoked by ouabain was examined. We focused on the involvement of three types of voltage-dependent Ca^{2+} channel, the L- and N types in the NA release evoked by ouabain. Sixty minutes after starting local administration of verapamil (100 μM), or ω-conotoxin GVIA (10 μM), we measured the ouabain-induced NA response. Second, we examined the involvement of plasma membrane Na^+/Ca^{2+} exchanger in the NA release evoked by ouabain. The inhibitors of membrane Na^+/Ca^{2+} exchange (dechlorobezamil; 100 μM, or KB7943; 10 μM) were locally administered through the dialysis probe and the ouabain-induced NA response was measured. Third, we examined the involvement of intracellular Ca^{2+} level in the NA release evoked by ouabain. An intracellular Ca^{2+} antagonist [3,4,5-trimethoxybenzoic acid 8-(dietyl amino)-octyl ester (TMB-8)] blocks the efflux of calcium from intracellular calcium stores without affecting influx

 doi: 10.1111/j.1748-1716.2007.01749.x

(Wiedenkeller & Sharp 1984). TMB-8 (1 mM) was locally administered through the dialysis probe and ouabain-induced NA response was measured. A similar pharmacological intervention was performed and ouabain-induced ACh responses were measured. Sixty minutes after starting local administration of verapamil (100 μM), or ω-conotoxin GVIA (10 μM), ω-conotoxin MVIIC (10 μM), we measured the ouabain-induced ACh response. The inhibitor of membrane Na^+/Ca^{2+} exchange (KB7943; 10 μM) was locally administered through the dialysis probe and the ouabain-induced ACh response was measured. Third, an intracellular Ca^{2+} antagonist (TMB-8, 1 mM) was locally administered through the dialysis probe and ouabain-induced ACh response was measured.

Analytical procedure

Dialysate NA concentrations were measured by HPLC with electrochemical detection (HPLC-ECD; Eicom, Kyoto, Japan). An alumina procedure was performed to remove the interfering compounds from the dialysate. The detection limit was 50 fmol per injection. Dialysate ACh concentration was measured directly by another HPLC-ECD. The detection limit was 50 fmol per injection. Details of HPLC-ECD for the NA and ACh measurements have been described elsewhere (Akiyama *et al.* 1991, 1994).

At the end of each experiment, the cats were killed with an overdose of pentobarbital sodium, and the implant sites were checked to confirm that the dialysis probes had been implanted within the left ventricular myocardium. Statistical analysis of the data was performed by analysis of variance (ANOVA). Statistical significance was defined as $P < 0.05$. Values are presented as mean ± SE.

Results

Protocol 1: Time course of dialysate NA and ACh levels during local administration of ouabain

Although local administration of ouabain did not affect haemodynamic parameters including heart rate, mean arterial pressure and electrocardiogram, ouabain induced the efflux of NA. Figure 1 (upper panel) shows the time course of the dialysate NA levels during local administration of ouabain (100 μM). Dialysate NA level increased significantly from 0.18 ± 0.06 nmol L^{-1} at control to 2.39 ± 0.53 nmol L^{-1} at 10, 12.92 ± 1.39 nmol L^{-1} at 20 min and 14.79 ± 1.97 nmol L^{-1} at 30 min. Subsequently, a slow decline occurred but high dialysate NA levels were maintained during locally applied ouabain. Peak level of dialysate NA ranged from 20 to 30 min after the beginning of ouabain administration. Figure 1 (lower panel) shows the time course of the dialysate ACh levels during local administration of ouabain (100 μM). Dialysate ACh level increased significantly from 0.91 ± 0.05 nmol at control to 3.6 ± 0.60 nmol L^{-1} at 0–15, 8.1 ± 1.4 nmol L^{-1} at 15–30 min and 6.8 ± 1.25 nmol L^{-1} at 30–45 min. Peak level of dialysate ACh appeared at 15–30 min after the beginning of ouabain administration.

Protocol 2: Influence of denervation and TTX on dialysate NA and ACh responses evoked by ouabain

We sampled the dialysates over 60 min of ouabain administration. To compare ouabain-induced NA or ACh levels under various interventions, ouabain-induced dialysate NA or ACh levels were subtracted from the control values. The sum of relative changes in dialysate NA or ACh (the unit: Σnmol/L) was expressed as an index of total NA or ACh release evoked by ouabain. Figure 2 (upper panel) shows the total NA release evoked by ouabain when cardiac sympathetic nerves were either intact, transected, pretreated with TTX. The ouabain-induced total NA release did not differ among them. Figure 2 (lower panel) shows the total ACh release evoked by ouabain when cardiac parasympathetic nerves were either intact, transected, or pretreated with TTX. The ouabain-induced total ACh release did not differ between the intact cardiac parasympathetic nerve and denervated groups whereas addition of TTX significantly inhibited the total ACh release by approx. 57% of vehicle.

Protocol 3: Influence of transport blocking agents on dialysate NA and ACh responses evoked by ouabain

Figure 3 (upper panel) shows the total NA release evoked by ouabain among various pharmacological interventions. Pretreatment with reserpine caused significant augmentation of the ouabain-induced total NA release whereas pretreatment with desipramine caused significant suppression of the total NA release. Figure 3 (lower panel) shows the total ACh release evoked by ouabain among various pharmacological interventions. The ouabain-induced total ACh release did not differ between the intact and hemicholinium-3 pretreated groups whereas addition of vesamicol significantly inhibited the total ACh release by approx. 45% of vehicle.

Protocol 4: Influence of Ca^{2+} mobilization on dialysate NA and ACh responses evoked by ouabain

Figure 4 (upper panel) shows the total NA release evoked by ouabain among various Ca^{2+} interventions. The total NA release in the 60 min after administration

Journal compilation © 2007 Scandinavian Physiological Society, doi: 10.1111/j.1748-1716.2007.01749.x

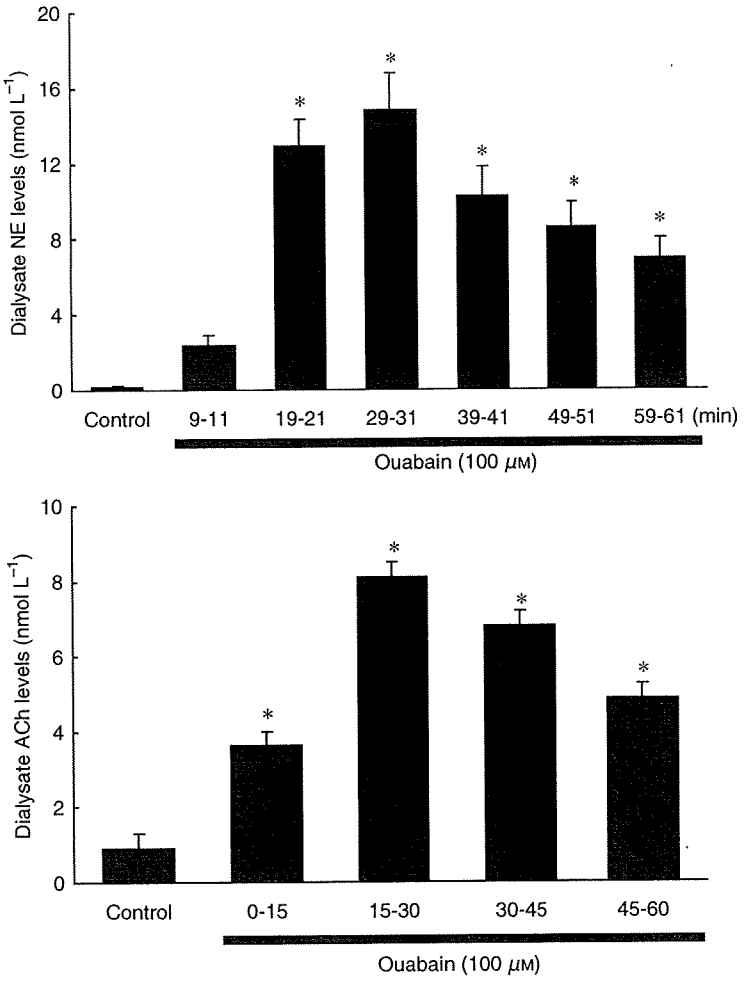

Figure 1 Upper panel: Time course of dialysate noradrenaline (NA) levels during local administration of ouabain (100 μM). Ouabain increased the dialysate NA levels. Subsequently, a slow decline occurred but high NA levels were maintained. Lower panel: Time course of dialysate acetylcholine (ACh) levels during local administration of ouabain (100 μM). Ouabain increased the dialysate ACh levels. Subsequently, a slow decline occurred but high ACh levels were maintained. Values are presented as the mean ± SE (for each column $n = 6$) *$P < 0.05$ vs. control.

of ouabain was significantly suppressed by approx. 47% and 55% of vehicle by addition of verapamil and ω-conotoxin GVIA. Pretreatment with TMB-8 caused significant suppression of the ouabain-induced total NA release whereas pretreatment with neither KB-7943 nor dechlorobezamil altered the total NA release. Figure 4 (lower panel) shows the total ACh release evoked by ouabain among various Ca^{2+} interventions. The total ACh release in the 60 min after administration of ouabain was significantly suppressed by approx. 57% of vehicle by addition of ω-conotoxin MVIIC. Pretreatment with neither verapamil nor ω-conotoxin GVIA altered the total ACh release. Pretreatment with TMB-8 caused significant suppression of the ouabain-induced total ACh release whereas pretreatment with KB-7943 did not alter the total ACh release.

Discussion

The present study indicates that in an *in vivo* preparation, ouabain alone induced NA or ACh release from sympathetic or parasympathetic nerve endings respectively. This discussion addresses mainly similarities and differences in ouabain alone induced NA or ACh releasing sites and mechanisms.

Regional depolarization evoked by ouabain

At the post-ganglionic nervous endings, ouabain induced NA and ACh release. The transection of sympathetic or parasympathetic nerve did not affect the amount of NA or ACh release evoked by ouabain. After the transection of cardiac sympathetic or parasympathetic nerves, ouabain at 100 μM induced increases in dialysate NA or ACh levels, which were as much as those evoked by electrical stimulation of the autonomic nerve (Akiyama *et al.* 1994, Yamazaki *et al.* 1997). These data suggest that ouabain itself induces regional depolarization following exocytosis. In the case of locally administered ouabain, ouabain produced intracellular Na^+ accumulation evoked by the inhibition of Na^+,K^+-ATPase (Mclvor & Cummings 1987).

